MSDE

PAPER

View Article Online
View Journal

Cite this: DOI: 10.1039/d6me00011h

Overcoming expression bottlenecks in recombinant silk–elastin-like polypeptides *via* plasmid backbone and protein engineering approaches

Andrea Andersson Rodriguez,†[ab] Ruiyan Gao,†[ab] Ebony Shire[ab] and Diego López Barreiro *[ab]

Silk–elastin-like polypeptides (SELPs) are sustainable recombinant biopolymers with applications in tissue engineering, drug delivery, or biosensing, to name a few. In contrast to the synthesis of traditional fossil-based polymers, SELPs are encoded by DNA, which leads to reproducible sequences and molecular weights. However, large-scale production of SELPs is hindered by the typical low yields attained in microbial expression systems. This is often attributed to (i) expression challenges caused by the repetitive nature of silk- and elastin-like tandem repeats in the SELP sequence, which can reduce ribosome processivity or cause mRNA instability through secondary structure formation; and (ii) cellular toxicity caused by SELP aggregation or inclusion body formation, particularly through irreversible aggregation of silk-like blocks. Here, we investigate strategies to prevent those limitations and enhance the heterologous expression of a positively charged SELP in *Escherichia coli* by systematically evaluating modifications at both the plasmid backbone and protein engineering levels. Plasmid backbone modifications encompass different antibiotic resistance markers (ampicillin *vs.* kanamycin), promoter switching (T7 *vs.* pBAD) and upregulation of glycine tRNA production. Protein engineering modifications included reducing molecular weight (from 57.5 to 38.5 kDa), varying the number of consecutive silk-like blocks (2, 4 or 8), and incorporating an N-terminal AKTK expression tag. Plasmid backbone modifications alone did not improve expression beyond its baseline yield (7.3 ± 3.1 mg L^{-1}). In contrast, adding an N-terminal AKTK tag alleviated translation bottlenecks and increased expression by 8.5-fold, independent of the number of consecutive silk-like blocks or the SELP molecular weight. Notably, alleviating this translation bottleneck enabled additional plasmid backbone optimisation strategies to further improve expression. As an example, the combined effect of adding an N-terminal AKTK tag plus upregulating glycine tRNA production resulted in a cumulative 17.0-fold improvement. Collectively, these findings highlight the critical role of N-terminal sequence engineering in unlocking efficient SELP translation and expression.

Received 21st January 2026,
Accepted 2nd June 2026

DOI: 10.1039/d6me00011h

rsc.li/molecular-engineering

Design, System, Application

Natural structural proteins – such as elastin, silk and collagen – inspire the design of protein-based materials for applications in healthcare, textiles and adhesives. These proteins often contain repetitive amino acid building blocks, also known as tandem repeats, that govern their self-assembly and their mechanical, structural and dynamic properties. Recombinant DNA technology enables design of new nature-inspired polypeptides that combine building blocks from different structural proteins to create sequences beyond those selected by evolution. This modular strategy provides a platform for creating multifunctional protein-based materials that blend properties from various natural proteins, such as in silk–elastin-like polypeptides (SELPs). SELPs fuse the strength of silk, contributed by GAGAGS blocks, with the elasticity and stimuli-responsiveness of elastin, conferred by VPGXG blocks. As DNA synthesis becomes increasingly cheap, achieving efficient protein expression and optimising yields become the main bottleneck for scaling production, reducing costs and accelerating the adoption of protein-based materials. Here, we explore how to achieve high-yield microbial production of SELPs by systematically evaluating the effect of modifications at the plasmid level (promoters, antibiotic markers, glycine tRNA supply) and the protein level (molecular weight, silk block arrangement, N-terminal tags). Overall, our results provide molecular engineering insights for optimising the expression of recombinant structural proteins.

Introduction

As the environmental and economic costs of fossil fuel-derived plastics continue to rise, there is an urgent demand for sustainable alternatives. Conventional polymers persist in ecosystems for centuries, damaging wildlife and contributing

[a] *Manufacturing Futures Lab, Department of Chemical Engineering, University College London, London, WC1E 7JE, UK. E-mail: d.lopezbarreiro@ucl.ac.uk*
[b] *Centre for Nature-Inspired Engineering, Department of Chemical Engineering, University College London, London, WC1E 7JE, UK*
† These authors contributed equally to the work.

significantly to environmental degradation.[1] Meanwhile, the global demand for synthetic polymers continues to grow rapidly, with an estimated compound annual growth rate of 7.0% and a market volume that is set to expand to $46.08 billion by 2029.[2] These growing figures underscore the urgent need for eco-friendly solutions that meet the demand for polymers in an environmentally conscious way. This has catalysed interest in biodegradable, bio-derived polymers that can support a circular economy. Among emerging materials, protein-based biopolymers offer a particularly attractive alternative due to their biodegradability, tuneable properties, and compatibility with biological systems.[3] Additionally, these materials are lightweight, easily processed, and responsive to environmental stimuli.[4]

Natural structural proteins such as silk, elastin, squid ring teeth and resilin serve as excellent templates for the design of advanced materials, with promising applications across fields such as biomedicine, food packaging, and soft robotics.[5–9] However, most structural proteins are difficult and uneconomical to harvest from nature. In turn, bioprocesses allow for high-fidelity bioproduction of recombinant proteins – including proteins beyond those selected for by evolution – using microbial fermentations. One example of the latter are silk–elastin-like polypeptides (SELPs). These hybrid polypeptides contain both elastin- and silk-like tandem repeats inspired by the sequences of human tropoelastin and silkworm silk, respectively.[10] Elastin-like blocks (VPGXG, with X being any amino acid besides proline[11]) promote the thermoresponsive self-assembly of SELPs above a transition temperature (T_t), whereas silk-like blocks form β-sheets that provide mechanical strength to SELP-based materials. These materials have been used for applications such as tissue engineering, drug delivery, injectable therapies, biosensing, or smart materials.[7,12–20]

On the one hand, the thermoresponsiveness of SELPs is promising for their scalable production because it enables non-chromatographic purification *via* reversible phase transitions, simplifying downstream processing and potentially improving economic feasibility.[21] On the other hand, producing SELPs recombinantly is non-trivial[22,23] due to the genetic instability associated with their repetitive sequences, which can lead to transcriptional errors, low expression yields, premature translation termination,[24] strain to the host cell's translation machinery, and even toxicity to cells in some instances.[25] Additional bottlenecks involve tRNA pool depletion, plasmid instability, high molecular weight (MW) or hydrophobicity.[26,27]

The bioproduction of SELPs has been demonstrated in several *E. coli* strains, such as BL21 (DE3),[18,28–30] BLR[31–33] or K12,[34,35] typically using T7-based expression systems with ampicillin or kanamycin selection and IPTG induction. In those studies, the reported yields varied widely, from typically <100 mg L^{-1} in shake flasks to 1–10 g L^{-1} in bioreactors (see Table S1). Several studies have analysed the influence of bioprocessing parameters (*e.g.*, expression temperature, media, pre- and postinduction growth rates, cell density at induction, antibiotic stability, dissolved oxygen, inducer concentrations and agitation) on the expression of SELPs using *E. coli* BL21 (DE3).[28,30,36] Beyond bioprocess optimisation approaches, plasmid backbone and protein engineering strategies provide another avenue to increase the yields of recombinant structural proteins by alleviating host burden and reducing protein aggregation. Typical modifications include codon optimisation, adjustment of silk-to-elastin ratios, changes in promoter system, or the incorporation of solubility tags.[26,37–42]

In this manuscript, we systematically explored how plasmid backbone and protein engineering modifications influence the bioproduction of highly repetitive SELPs in *E. coli*. The aim was to overcome low-yield bottlenecks and reduce overall production costs – aspects that are critical for SELPs to reach competitiveness with conventional fossil-derived polymers. Modifications involving the antibiotic resistance marker (ampicillin *vs.* kanamycin), promoter (T7 *vs.* pBAD) or glycine tRNA upregulation, did not led to measurable improvements in protein yields ($\sim$7.3 mg L^{-1}). In turn, incorporating an N-terminal AKTK tag while supplementing glycine tRNA resulted in a cumulative 17.0-fold improvement. Other protein engineering modifications, including the reduction in molecular weight (MW) from 57.5 to 38.5 kDa, or a rearrangement of silk-like blocks (2, 4 or 8) did not lead to further improvements beyond that provided by the addition of the N-terminal AKTK tag. Overall, the results highlight the benefits of N-terminal tags and glycine tRNA supplementation for enhancing the yields of microbially produced SELPs.

Materials and methods

Plasmid and protein design

Synthetic biology and protein engineering modifications were investigated to enhance the yields of three positively charged SELPs (Fig. 1). Their MW, isoelectric point (pI) and Kyte–Doolittle hydrophobicity[43] were obtained as theoretical estimates based on the primary amino acid sequences using the Expasy server.[44] The codon adaptation index (CAI) was computed for the nucleotide sequences of the three SELPs using the CAI tool from the European Molecular Biology Open Software Suite (EMBOSS). This tool quantifies how closely the codon usage of a gene (in this case, encoding for a SELP) matches that of highly expressed genes in *E. coli*. CAI values were calculated using the Eecoli_high.cut codon-usage table, which is recommended for analyses focused on translational efficiency. The full amino acid sequences and plasmid maps are included in Table S2 and Fig. S1. The plasmid encoding for S8E58-K with a T7 promoter and ampicillin resistance was used as baseline system. This system was subjected to various modifications, whose rationale is detailed in Table 1.

Plasmid backbone modifications

All plasmid backbone modifications (Table S3) were performed using standard molecular biology techniques.

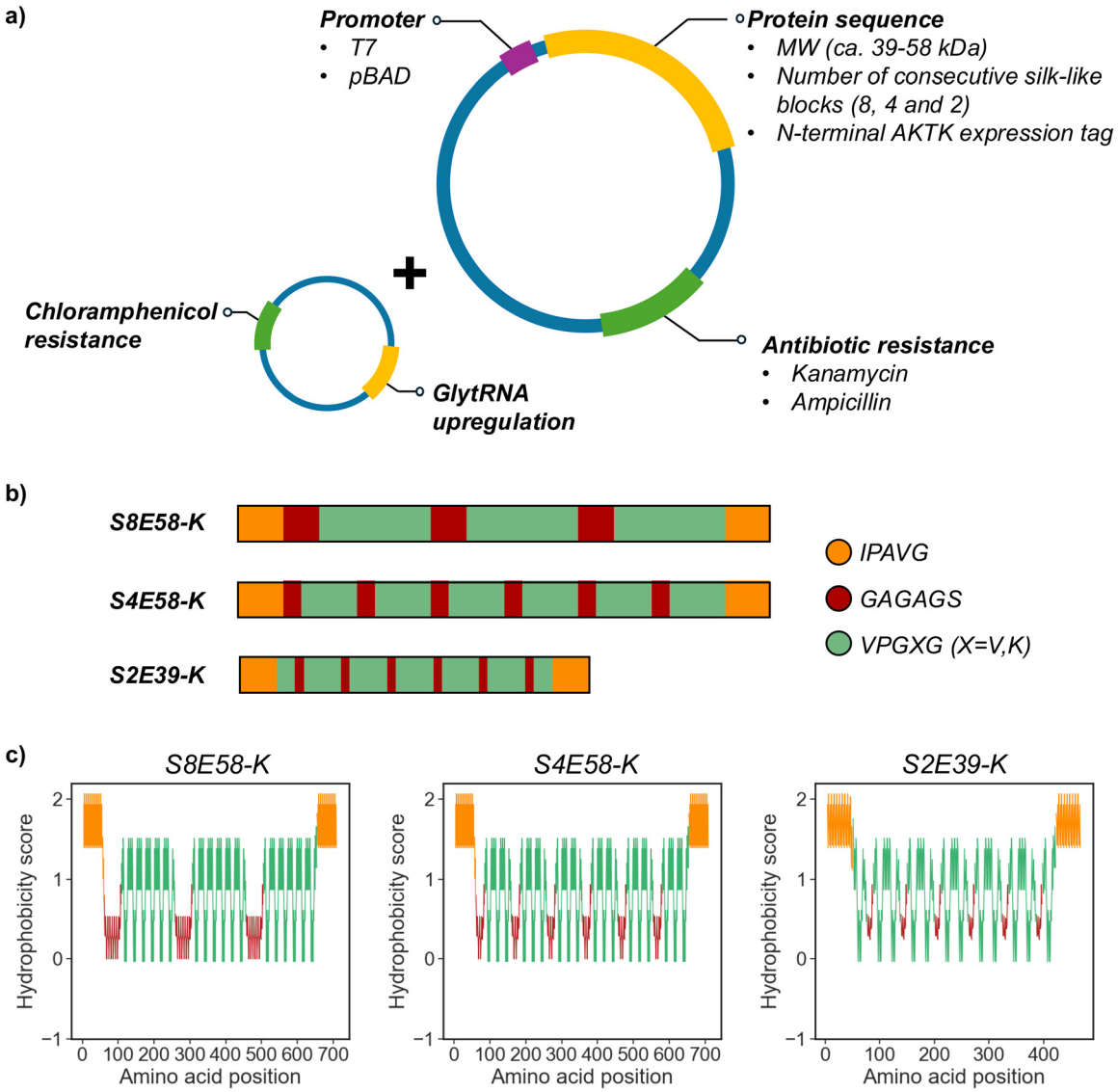

Fig. 1 (a) Plasmid backbone (promoter, selection system, GlytRNA upregulation) and protein engineering modifications (distribution of silk-like blocks and MW reduction) investigated in this study. (b) Schematic representation of the distribution of building blocks along the sequences of the SELP library discussed in this study; (c) hydropathy plots as calculated using the Kyte–Doolittle scale, colour-coded as in (b).

Restriction enzyme digestions and ligation reactions were conducted according to the manufacturers' recommended protocols. Plasmid and genomic DNA from *E. coli* were purified using Qiagen kits (Qiagen, Germany). Amplified fragments and ligation products were verified by agarose gel electrophoresis on 0.8% agarose (Bio-Rad, Spain) in 1× TAE

Table 1 Summary of plasmid backbone and protein engineering modification strategies to enhance silk–elastin-like polypeptide yields

Strategy	Modification type	Rationale
Plasmid backbone modifications	Antibiotic selection marker	Improve plasmid stability
	Promoter	Weaker promoter reduces metabolic burden Improve protein folding and accumulation
	Co-expression of GlytRNA upregulating plasmid	Reduce codon bias effects Enhance translation
	N-terminal tag	Improve translation initiation
Protein engineering modifications	Shorter MW	Reduce translation time Reduce metabolic burden
	Silk-like block redistribution	Reduce β-sheet formation Reduce aggregation Reduce metabolic burden on host cell

buffer, with GelRed® staining (Sigma-Aldrich, UK). PCR samples and agarose gel extractions were cleaned up using Wizard® SV Gel and PCR Clean-Up System kit (Promega, UK). Primers for PCR and sequencing were synthesised by Thermo Fisher Scientific (UK) (Table S4). All constructed plasmids were verified by Sanger sequencing performed by Azenta Life Sciences (UK).

- *Baseline expression plasmid:* the SELP termed S8E58-K (57.5 kDa) was designed as the baseline construct. This polypeptide contained elastin-like blocks (IPAVG, VPGVG, VPGKG) and silk-like blocks (GAGAGS) and possessed a net positive charge due to the incorporation of lysine (K) residues as the X residue in some of the elastin-like blocks. Synthetic DNA encoding for the full length of S8E58-K was synthesised by GeneArt (Regensburg, Germany) and cloned into the Champion™ pET303/CT-His vector (ThermoFisher, UK) between the *Xba*I and *Xho*I restriction sites. Each sequence terminated with two stop codons (TAATAA) to ensure proper translational termination[45] and avoid the translation of the HisTag encoded after the *Xho*I restriction site. Controlled by the T7 promoter system and carrying an ampicillin selection marker (Amp), this construct served as the baseline for assessing the impact of alternative engineering strategies on protein expression.

- *Kanamycin-selectable expression plasmid:* to assess the influence of selection marker on expression efficiency, S8E58-K was cloned into a kanamycin-resistant backbone. This plasmid, synthesised by GenScript Biotech (UK), retained the same promoter and regulatory elements as the baseline construct, except that a kanamycin resistance gene replaced the original ampicillin resistance gene.

- *Arabinose-inducible expression plasmid:* to investigate the effect of promoter type, a new plasmid was synthesised by GenScript Biotech (UK), placing S8E58-K expression under the control of the arabinose-inducible pBAD promoter within a kanamycin-selectable backbone.

- *Glycyl tRNA overexpression plasmid:* to assess the effect of glycyl tRNA (GlytRNA) availability on translational efficiency, a secondary plasmid pACYC184_glyVXY, was constructed as reported elsewhere.[46] This construct increased intracellular GlytRNA levels through expression of the glyVXY operon under its native promoter. Genomic DNA from *E. coli* BW25113 was used as template for PCR amplification of the glyVXY operon using Q5® High-Fidelity DNA Polymerase (New England Biolabs, UK), following the manufacturer's protocol, and primers FglyEco and RglyBam (Table S4). The PCR product and pACYC184 vector (Cambridge Bioscience, UK) were digested with *Eco*RV (Promega, UK) and *Bam*HI (Thermo Fisher, UK), and ligated using T4 DNA Ligase (New England Biolabs, UK).

- *N-terminal AKTK tag:* to determine whether a short N-terminal peptide could alleviate translation stalling at the start of the S8E58-K sequence, a plasmid encoding the AKTK peptide (5′-GCCAAAACCAAA-3′) immediately downstream of the start codon was generated.[26,41] The S8E58-K plasmid with kanamycin resistance was PCR-amplified with primers Fwd_AKTK and Rev_AKTK (Table S4) to insert the AKTK tag. The resulting PCR product insert was then re-circularised using the In-Fusion® Snap Assembly kit (Takara Bio, USA) according to the manufacturer's protocol.

Protein engineering modifications

Two variants of the S8E58-K construct with N-terminal AKTK tag were tested:

- *Variant with redesigned silk block distribution:* to evaluate the effect of consecutive silk-like blocks, a modified SELP construct S4E58-K was synthesised by GeneArt (Germany) and supplied already cloned into the Champion™ pET303/CT-His vector (T7 promoter, Amp resistance) between the *Xba*I and *Xho*I restriction sites. Compared to S8E58-K, the number of consecutive GAGAGS silk-like blocks in S4E58-K was reduced from 8 to 4, while maintaining the overall number of silk-like blocks and MW (Fig. 1b).

- *Variant with reduced molecular weight:* to examine the effect of MW on SELP expression, the S2E39-K gene was synthesised by GeneArt (Germany) and supplied already cloned into the Champion™ pET303/CT-His vector (T7 promoter, Amp resistance) between the *Xba*I and *Xho*I restriction sites. This sequence had a lower MW (38.5 kDa) and a reduced number of consecutive silk-like blocks (2) than S8E58-K and S4E58-K.

Cell transformation

Plasmid DNA was transformed into the *E. coli* strains BL21 (DE3) (New England Biolabs, UK), *E. coli* BL21 Star™ (DE3) (ThermoFisher, UK) or BLR (DE3) (Novagen, UK) competent cells *via* heat shock transformation. Briefly, 2 μL of plasmid DNA were combined with 25 μL of competent cells and incubated on ice for 30 min. The mixture was then heat shocked at 42 °C for 30 s and immediately returned to ice for 5 min. Subsequently, 250 μL of pre-warmed S.O.C. medium (Invitrogen™, USA) was added, and the cells were incubated at 37 °C with shaking at 250 rpm for 1 h. Following recovery, 50 μL of the transformation mixture was spread onto LB agar plates containing the appropriate antibiotics – 100 μg mL^{-1} ampicillin (Sigma-Aldrich, USA), 50 μg mL^{-1} kanamycin sulphate (Fluorochem Ltd., UK) or 25 μg mL^{-1} chloramphenicol (Sigma-Aldrich, USA) – and incubated overnight at 37 °C to allow colony growth.

Culturing conditions

Luria Broth (LB) (Invitrogen™, UK) and Terrific Broth (TB) media (Fisher Scientific, UK) were prepared following manufacturer's guidelines and sterilised by autoclaving at 121 °C for 15 minutes. Antibiotics were added based on the plasmids present (ampicillin 100 μg mL^{-1}, kanamycin 50 μg mL^{-1}, chloramphenicol 25 μg mL^{-1}). Overnight pre-cultures in 5 mL of LB medium were prepared from a glycerol stock formed from a single transformed colony, followed by incubation with shaking at 250 rpm overnight. Overnight pre-

cultures were diluted 1 : 100 into 500 mL of TB medium with appropriate antibiotics in 2 L shake flasks and grown at 37 °C and 200 rpm. SELP expression was induced at an OD of 0.6 *via* the addition of 1.0 mM IPTG (Sigma-Aldrich, USA) or 0.2% (w/v) L-arabinose (Apollo Scientific LTD, UK), depending on the promoter. Besides these standard conditions, a small set of additional experiments were carried out at lower induction temperatures (16 °C) or lower IPTG concentration (0.5 mM) to investigate if milder conditions could lead to reduced cellular stress and improved SELP expression. All cultures were performed at least in triplicate.

Cell harvesting

After induction, SELPs were expressed overnight for *ca.* 16 h and harvested by centrifugation at 5000 × *g* at 4 °C for 15 min using an Avanti™ JXN-26 centrifuge (Beckman Coulter, UK). Cell pellets were washed with 20 mL of 1× phosphate buffered saline (PBS) solution (Gibco™, UK) and further centrifuged at 5000 × *g* at 4 °C for 15 min. The supernatant was discarded, and cell pellets were stored at −20 °C until further use.

Protein purification

Inverse temperature cycling (ITC) was employed to purify SELPs (Fig. 2). This purification method consists of alternating hot and cold cycles that exploit the inherent LCST phase behaviour of SELPs.[21,47,48] Firstly, cell pellets were ruptured to enhance the release of SELPs by resuspending thawed cells in Milli-Q and subjecting the solution to ultrasonication with a Sonic Dismembrator Model 120 (Fisher Scientific™, UK) for 3 min (10 s on/off, 65% amplitude). The resulting lysate underwent acid treatment, adjusted to pH 4 with 1 M HCl (Merck, UK) and incubated at 4 °C for 30 min to denature and precipitate the majority of cell debris.[49] The lysate was then subjected to a cold cycle to remove cell debris by centrifugation at 5000 × *g* at 4 °C for 10 min. Subsequently, SELP aggregation was induced. To do so, the pH was first adjusted to 10.5 using 1 M NaOH (Honeywell, Sweden) to deprotonate the lysine. Following this, 2 M NaCl (Fisher Scientific™, UK) was added to the solution. Adjusting the pH to the pI of SELPs and adding NaCl lowered the T_t and enhanced aggregation, facilitating a more efficient phase separation and purification of SELPs.[50] Once SELPs phase separated, they were subjected to a hot cycle centrifugation at 5000 × *g* for 10 min at either 24 °C (S8E58-K and S5E57-K) or 42 °C (S2E39-K). The resulting pellet was resuspended with Milli-Q for the subsequent cold cycle. Overall, 4–6 cycles were performed to ensure complete removal of non-SELP material. The final pellet from the last hot cycle was resuspended in 10 mL of Milli-Q water. 10 μL of the solution was reserved for standardised SDS-PAGE analysis, and the rest was desalted using 3000 MWCO Amicon Ultra-15 centrifugal filter units (MilliporeSigma, UK), followed by resuspension in Milli-Q water, flash freezing, lyophilisation, and storage at −20 °C until further use.

Protein expression analysis

To assess the yield and consistency of SELP production across different constructs and conditions, quantitative and qualitative methods were employed.

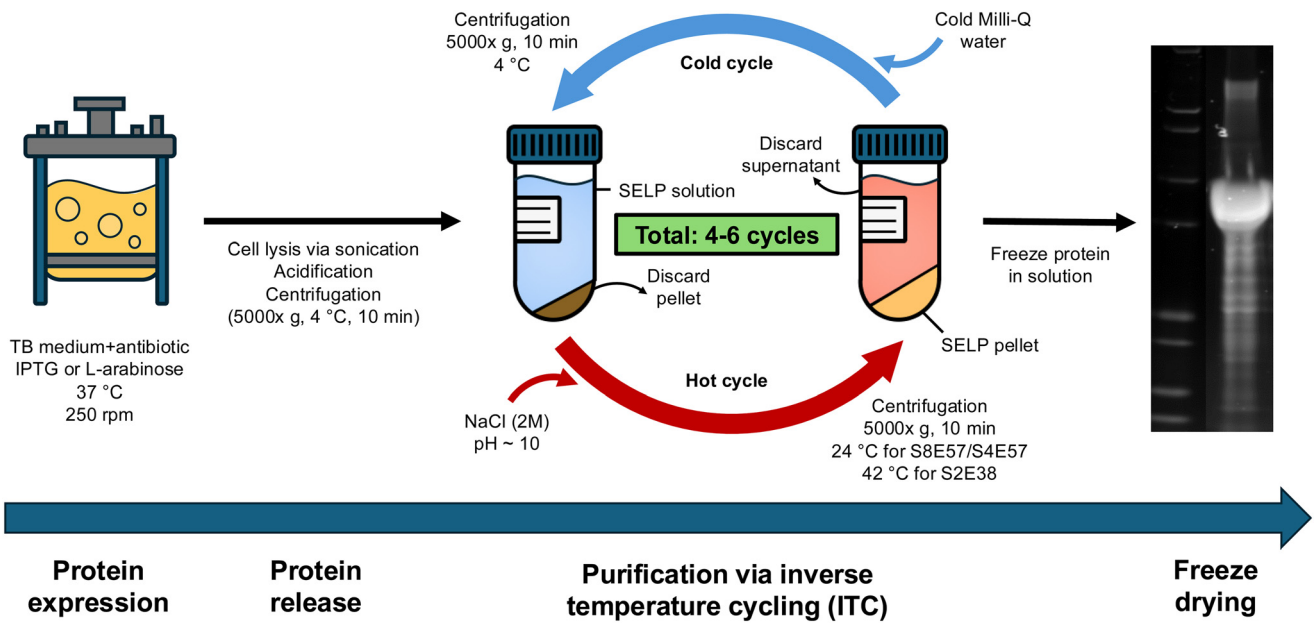

Fig. 2 Protocol for SELP purification, based on the inverse temperature cycling method. SELPs are purified by exploiting the reversible inverse thermoresponsiveness provided by elastin-like blocks. Heating above the transition temperature T_t induces SELP aggregation and phase separation (hot cycle), whereas cooling below T_t resolubilises the SELPs (cold cycle). Repeated heating–cooling cycles with centrifugation steps in between remove impurities without the need for chromatographic methods.

- *Dry weight:* protein yield (in mg L^{-1}) was quantified by weighing lyophilised protein obtained from 500 mL culture samples following purification. These yields provided a direct measure of the recovered protein mass yield for each construct under the specified expression conditions and were not corrected for purification losses.

- *Sodium dodecyl sulphate-polyacrylamide gel electrophoresis (SDS-PAGE):* NuPAGE 4–12% Bis-Tris gels (Invitrogen, UK) with 1× MOPS running buffer (Invitrogen, UK) were used, using Mark12™ Unstained Standard (Thermo Fisher, UK) as protein MW ladder. Due to the hydrophobic nature of most amino acids in the proteins expressed in this study, SYPRO Red (Invitrogen, UK) was used according to the manufacturer's instructions to stain SDS-PAGE gels. In this study, SDS-PAGE was primarily used to evaluate protein MW and purity. Relative expression levels were quantified *via* densitometric analyses using the software Fiji.[51] Importantly, densitometric comparisons were only performed between samples corresponding to the same SELP. This was a consequence of the staining mechanism of SYPRO Red, which preferentially binds exposed hydrophobic surfaces, making its staining efficiency depend strongly on protein disorder and conformationally flexibility. For SELPs, these properties vary substantially with sequence and block distribution, potentially leading to nonlinear staining responses across different constructs. It should also be noted that alanine-rich proteins like the SELPs in this study can show deviations of up to 20% between the theoretical MW of SELPs and their band position in SDS-PAGE gels.[49]

- *Presence of inclusion bodies:* to determine whether the expressed SELPs were aggregating into insoluble inclusion bodies,[52,53] cell pellets after denaturation at pH 4 and after the first cold cycle were solubilised in 8 M urea. This aimed at solubilising potential inclusion bodies following an adapted protocol.[54] Briefly, cold cycle pellets were resuspended in 20 mL of cold Milli-Q water and lysed by ultrasonication (3 min, 10 s on/off, 65% amplitude). Potential inclusion bodies were pelleted *via* centrifugation at 5000 × *g* for 10 min at 4 °C. 1 g wet weight of the pellet was washed with 9 mL of 8 M urea (Scientific Laboratory Supplies, UK) and incubated at room temperature with gentle rotation (80 rpm) for 1 h. Following centrifugation at 5000 × *g* for 20 minutes at 4 °C, 10 μL of supernatant containing fully denatured proteins was collected for SDS-PAGE analysis.

- *Matrix-Assisted Laser Desorption/Ionization Time-of-Flight Mass Spectrometry (MALDI-TOF MS):* MALDI-TOF MS spectra were acquired at the UCL Chemistry Mass Spectrometry Facility using a Shimadzu MALDI-8030 MS (Shimadzu, UK). The matrix consisted of sinapic acid (10 mg mL^{-1}) dissolved in water/acetonitrile (3 : 7, v/v). SELP samples were also dissolved in water/acetonitrile (3 : 7, v/v) at a concentration of 0.8 mg mL^{-1} and mixed with the matrix in a 2 : 5 (v/v) sample-to-matrix ratio containing 2% formic acid. Aliquots (2 μL) were spotted onto the MALDI target plate and air-dried. Data was acquired in linear positive mode over an *m*/*z* range of 10 000 to 100 000 with 120 laser shots per spectrum, pulsed extract at 57 000, and blanking mass 10 000, on 1 spot (rastered) for 10 shots accumulate at 200 Hz laser replicate rate.

- *Quantitative Reverse Transcription Polymerase Chain Reaction (RT-qPCR):* total bacterial RNA was extracted from cultures harvested 21 h post-induction, using a cell input equivalent to 1 mL of culture at OD_{600} = 2. Total RNA was isolated using the Aurum Total RNA Mini kit (Bio-Rad) according to the manufacturer's instructions. Following extraction, residual DNA was removed using the TURBO DNA-free kit (Thermo Fisher Scientific), and RNA concentration was assessed using a NanoDrop Eight spectrophotometer (Thermo Scientific). cDNA was synthesised using the iScript cDNA Synthesis kit (Bio-Rad) in 20 μL reactions containing 500 ng of total RNA. Reverse transcription was performed according to the manufacturer's protocol: priming at 25 °C for 5 min, reverse transcription at 46 °C for 20 min, followed by reverse transcriptase inactivation at 95 °C for 1 min. Relative mRNA levels were quantified using a QuantStudio 1 Real-Time PCR System. The BL21 16S rRNA gene was used as the housekeeping reference gene, and its genomic DNA sequence was obtained from the NCBI Nucleotide database.[55] qPCR reactions were performed using iTaq Universal SYBR Green Supermix (Bio-Rad). The amplification programme consisted of polymerase activation and initial denaturation at 95 °C for 30 s, followed by 40 cycles of amplification (95 °C for 15 s and 62 °C for 60 s). Melt-curve analysis was performed from 65 °C to 95 °C after amplification to confirm the presence of a single amplified product. Ct values were determined from the exponential phase of amplification. Relative expression levels were calculated by normalising the Ct value of the target SELP gene to that of the 16S reference gene to obtain ΔCt values. Fold changes were then calculated using the $2^{-\Delta\Delta Ct}$ method.[56] RT-qPCR analysis was performed using three biological replicates, each analysed with three technical replicates.

Statistical analysis

All statistical analyses were performed in Python using SciPy and Statsmodels. Group means were compared using a 2-sided Welch's *t*-test, which does not assume equal variances between groups.[57] For each group, results are reported as the mean ± standard deviation (SD) from $n = 3$ biological replicates, as well as 95% confidence interval (CI) calculated using the *t*-distribution. The significance level is depicted in the figures as * ($p < 0.05$), ** ($p < 0.01$) and ns (not significant). In addition to *p*-values, effect sizes were reported as Hedges' *g*, using a small-sample correction. Groups with zero variance (no detectable expression) were not subjected to statistical testing. Given the small sample size ($n = 3$ biological replicates per group), we assessed statistical sensitivity by estimating the minimum detectable effect size (MDE) at 80% power and $\alpha = 0.05$.

Results and discussion

E. coli strain selection

A survey of the literature regarding bioproduction of ELPs and SELPs (which are most commonly purified *via* ITC)

showed no consistent trends regarding the optimal host strain for SELP expression[40,42] (Table S1). Thus, we first evaluated three *E. coli* DE3 strains – BL21, BL21 Star™ and BLR – commonly used for SELP production. BL21 is a commonly used host for recombinant protein expression, whereas BL21 Star™ and BLR have features that might be useful for the expression of highly repetitive proteins: BL21 Star™ is engineered to enhance mRNA stability and BLR is reported to exhibit enhanced plasmid stability and reduced recombination. Here, these strains were tested for the expression of S8E58-K using the baseline vector, which consisted of a pET303-CT/His plasmid with a T7 promoter and ampicillin resistance. During ITC purification, lysates from all three strains showed minimal turbidity, suggesting low SELP expression in those systems. Indeed, SDS PAGE analysis revealed only minor differences in the intensity of the S8E58-K bands across strains (Fig. 3a). Additionally, a densitometry analysis of the gel confirmed the absence of statistically significant differences in expression levels (Fig. 3b). Based on these results and the reported enhanced mRNA stability for BL21 Star™, we selected this strain for subsequent experiments.

Previous studies on silk-like polypeptides and SELPs reported up to a 5-fold increase in expression when shifting induction temperatures from 37 °C to 16 °C in T7-based pET28a systems, attributed to increased solubility and a reduced amount of truncated transcripts.[27,58] However, although low-temperature induction is frequently promoted as a strategy for enhancing recombinant protein production, its effectiveness is highly protein-dependent. In our case, induction at 16 °C did not increase S8E58-K yields, agreeing with previous reports that showed enhanced expression of SELPs at temperatures between 37–42 °C.[30,36] We also searched for the presence of S8E58-K inclusion bodies by resolubilising the pellets obtained after acidification at pH 4 and after the first hot cycle using urea 8 M. If S8E58-K was being lost *via* inclusion bodies, we should observe an overexpressed band in SDS PAGE gels when resolubilising those pellets. However, the lack of any overexpressed bands indicated that inclusion bodies were not a major source of losses during S8E58-K production or purification. Overall, the marginal variations in S8E58-K expression caused by changes in the induction temperature or the absence of S8E58-K inclusion bodies underscored the need for plasmid backbone or protein engineering modifications to enhance protein yields.

Plasmid backbone and protein engineering modifications for high-yield SELP expression

In an attempt to increase the yields of S8E58-K, we explored modifications at the plasmid backbone level (promoter and selection system or upregulation of GlytRNA), as well as protein engineering modifications (sequence architecture and molecular weight). The following sections discuss the effect of these modifications on the S8E58-K yields (Fig. 4). Full details of individual replicas and a detailed statistical analysis are provided in the SI (Tables S5 and S6). Additionally, the MW of proteins containing an N-terminal AKTK tag was characterised *via* MALDI-TOF MS to confirm intact protein expression (Fig. S2–S4). The experimental

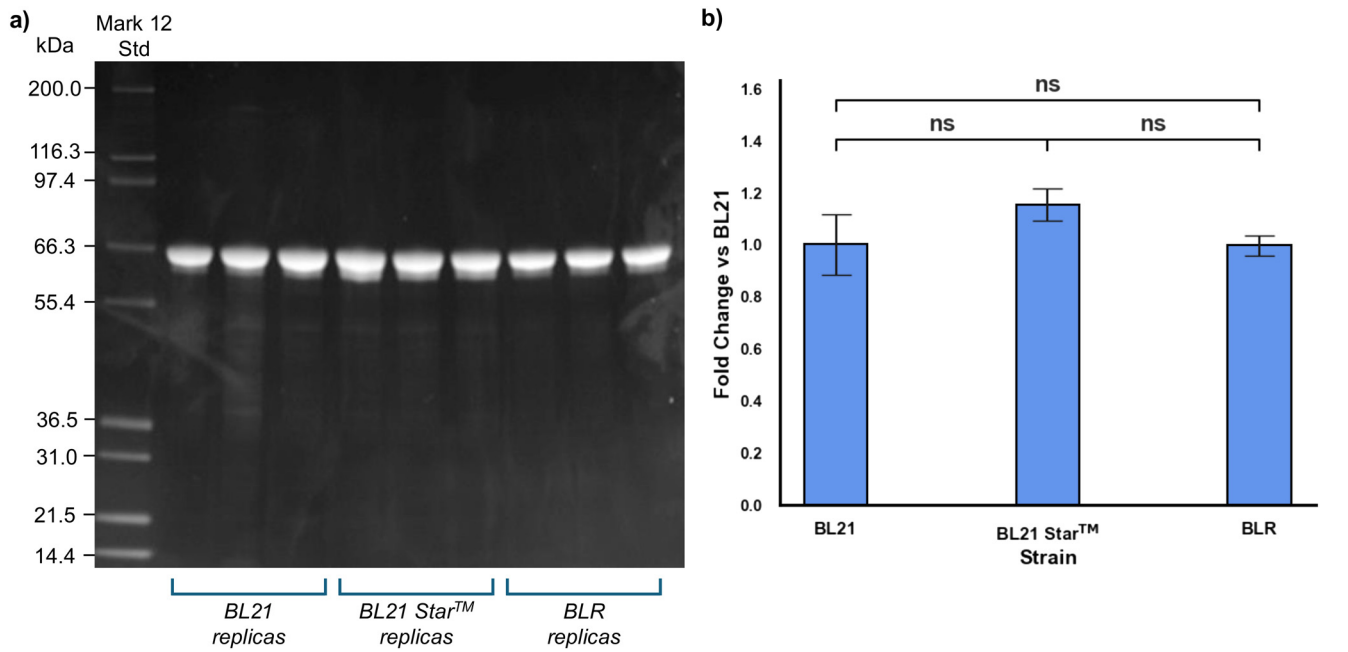

Fig. 3 S8E58-K yields with different *E. coli* DE3 strains. (a) SDS-PAGE analysis of S8E58-K expressed in *E. coli* using the S8E58-K_T7_Amp vector. Each lane contained 10 μL of the final purified SELPs dissolved in 10 mL Milli-Q water; lanes 1–3: biological replicates in BL21; lanes 4–6: biological replicates in BL21 Star™; lanes 7–9: biological replicates in BL21 BLR. (b) Densitometric analysis of the SDS-PAGE results for the various *E. coli* strains tested.

values were in good agreement with the theoretical MWs for the three SELPs tested in this study (Table 2), with low deviations ranging from 0.4 to 1.2%. To benchmark our results to the available literature (Table S1), yields reported in this study were measured in mg of SELP per L of culture. OD_{600} was not monitored after induction and therefore biomass-normalised productivities are not reported. Nonetheless, all constructs reported in this study showed similar growth prior to induction, and no noticeable differences in pellet size were detected after harvesting. This indicates that variations in expression yield discussed in the following sections are expected to reflect differences in expression efficiency rather than in biomass accumulation.

a) Plasmid backbone modifications.

- *Ampicillin vs. kanamycin:* the antibiotic resistance marker in the S8E58-K_T7_Amp plasmid was switched from ampicillin to kanamycin to make the plasmid S8E58-K_T7_Kan. This was based on the tendency of ampicillin to degrade over time and reduce selective pressure, and kanamycin's greater stability, which we hypothesised could enhance plasmid retention and improve S8E58-K yields.[59] Unfortunately, final dry weight measurements (Fig. 4) showed no statistically significant increase in S8E58-K yields when comparing ampicillin- and kanamycin-based constructs (7.3 ± 3.1 and 8.1 ± 2.9 mg L^{-1}, respectively), with SDS PAGE showing comparable purities (Fig. S5). However, although no immediate yield improvement was observed, kanamycin was

a)

SELP	Yield	Promoter	Resistance marker	GlytRNA upregulation	N-terminal AKTK tag	Consecutive silk-like blocks	MW (kDa)	Construct
S8E58	7.3 ± 3.1	T7	Amp	No	No	8	57.5	S8E58-K_T7_Amp
S8E58	8.1 ± 2.9	T7	Kan	No	No	8	57.5	S8E58-K_T7_Kan
S8E58	0.0	pBAD	Kan	No	No	8	57.5	S8E58-K_pBAD_Kan
S8E58	7.7 ± 0.3	T7	Kan	Yes	No	8	57.5	S8E58-K_T7_Kan + GlytRNA
S8E58	62.3 ± 9.9	T7	Kan	No	Yes	8	57.5	AKTK_S8E58-K_T7_Kan
S8E58	124.9 ± 20.2	T7	Kan	Yes	Yes	8	57.5	AKTK_S8E58-K_T7_Kan + GlytRNA
S4E58	62.06 ± 10.5	T7	Amp	No	Yes	4	57.5	AKTK_S4E58-K_T7_Amp
S2E39	67.7 ± 12.6	T7	Amp	No	Yes	2	38.5	AKTK_S2E39-K_T7_Kan

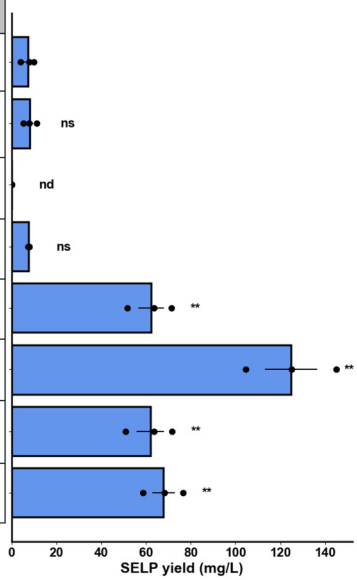

b)

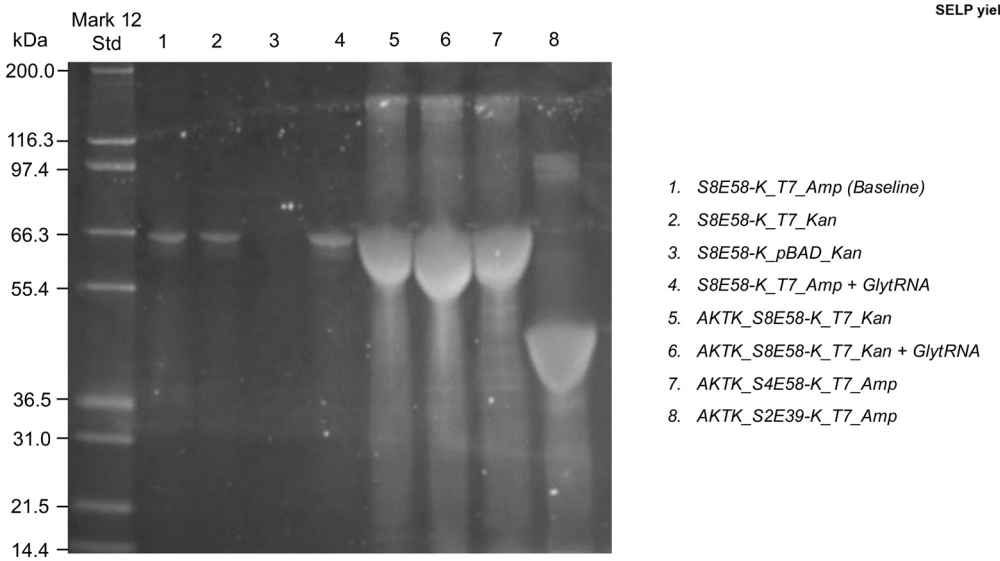

1. S8E58-K_T7_Amp (Baseline)
2. S8E58-K_T7_Kan
3. S8E58-K_pBAD_Kan
4. S8E58-K_T7_Amp + GlytRNA
5. AKTK_S8E58-K_T7_Kan
6. AKTK_S8E58-K_T7_Kan + GlytRNA
7. AKTK_S4E58-K_T7_Amp
8. AKTK_S2E39-K_T7_Amp

Fig. 4 Overview of plasmid backbone and protein engineering approaches to increase SELP yields. (a) Dry protein yields (mean ± SD, n = 3 biological replicates) for *E. coli* cultures transformed with the various plasmids encoding for S8E58-K, S4E58-K and S2E39-K. Statistical comparisons were made against the baseline construct S8E58-K_T7_Amp (see Tables S5 and S6) using two-sided Welch's t-tests. (b) SDS-PAGE results of the different plasmid modifications investigated in this work.

Table 2 MALDI TOF MS results of purified SELPs containing an N-terminal AKTK tag

SELP	Theoretical MW (Da)	Experimental MW (Da)
S8E58-K	57 933.4	57 221.5
S4E58-K	57 933.4	57 625.4
S2E39-K	38 919.7	38 772.6

used as preferred selection marker for the subsequent plasmid backbone modifications discussed in this manuscript. This was based on the established superior stability of kanamycin, which helps maintain selective pressure better than ampicillin, supporting plasmid stability and sustained protein expression over time.[36,60]

- *T7 vs. pBAD:* previous studies have shown that the T7 promoter system often exhibits leaky expression, a phenomenon we also observed in our experiments with varying IPTG concentrations (Fig. S6). This basal expression can impose metabolic stress on the host cells, potentially reducing protein yields due to toxicity.[42] In an attempt to mitigate this, we replaced the T7 promoter with the weaker, more tightly regulated pBAD promoter. The pBAD system has been reported to reduce the metabolic burden on host cells, allowing them to modulate protein synthesis in a more controllable fashion, which could potentially improve S8E58-K yields.[61] However, SDS-PAGE (Fig. S7) and final dry weight measurements (Fig. 4) showed no detectable expression of S8E58-K with the pBAD promoter, even after an increased number of replicas was performed. These results suggested that the pBAD promoter was too weak under the tested conditions, underscoring that the choice of promoter needs to balance tight regulation with sufficient transcriptional activity. Additionally, the rapid metabolism of the L-arabinose in *E. coli* BL21 Star™ could have also reduced induction efficiency.[62] Given these results, this pBAD promoter was not investigated further in this study, and subsequent tests were done with plasmid constructs containing the stronger T7 promoter.

- *Glycyl-tRNA overexpression:* the CAI value for S8E58-K was 0.453, indicating moderate adaptation to *E. coli* codon usage. When examining the codon usage specifically for glycine, S8E58-K contained predominantly GGC or GGT codons (~85%) (Fig. S8), which match the main GlytRNA isoacceptors in *E. coli*. Therefore, *a priori*, glycine incorporation should not be a limiting factor for S8E58-K expression. However, S8E58-K is a glycine-rich protein – glycine makes up 38.6% of its amino acids due to its silk-like (GAGAGS) and elastin-like (VPGXG/IPAVG) blocks. Because *E. coli* does not naturally overproduce glycine tRNAs,[63,64] we hypothesised that the high flux of glycine incorporation needed during S8E58-K translation could lead to a GlytRNA demand that exceeds the endogenous supply of *E. coli*, even with optimised glycine codon usage. This could impair translation efficiency, causing ribosomal stalling or premature termination. We therefore tested if supplementation with cognate tRNAs *via* overexpression of GlytRNA could improve S8E58-K yields, a strategy that was previously applied to other glycine-rich proteins, such as silk-like polypeptides.[26,27,46,58,64] Unfortunately, SDS-PAGE analysis (Fig. S9a) and final dry weight measurements (Fig. 4 and S10) revealed that runs with and without GlytRNA upregulation yielded comparable final protein yields (7.7 ± 0.3 mg L^{-1}). Furthermore, SDS-PAGE analysis confirmed that the protein migrated exclusively at its expected full length, with no detectable truncated forms. This indicated that S8E58-K was expressed in its intact form, suggesting that lack of translational completion was unlikely to be the primary barrier to higher yields.[42]

b) Protein engineering modifications.

- *Incorporation of N-terminal tag:* several literature reports suggest that the introduction of short N-terminal tags immediately after the start codon can enhance translation initiation rates for recombinant proteins, leading in some cases to 10-fold increases in protein yields. Moreover, enhanced translation initiation has been linked to stabilised protein synthesis, reduced mRNA degradation and decreased ribosome stalling.[65–67] For these reasons, we tested if incorporating an N-terminal tag could enhance SELP expression and thus alleviate expression bottlenecks. Several N-terminal tags – such as AMGGGA,[68] ESLLP[32,33] or AKTK[26,69,70] – can be found in the literature related to recombinant expression of structural proteins. Here, we chose the AKTK tag, because earlier reports suggested that small, less bulky residues near the start codon, such as alanine (A) in the second amino acid position, as well as threonine (T) and lysine (K), provide favourable codons for *E. coli* ribosomes.[41,71]

The addition of the N-terminal AKTK tag resulted in a marked improvement in S8E58-K expression. Quantitative analysis of dry weight confirmed an 8.5-fold increase in yield (62.3 ± 9.9 mg L^{-1}) compared to the baseline construct (Fig. 4), supported by a visibly more intense band on SDS-PAGE (Fig. S9b). Furthermore, combining the AKTK tag with co-expression of a GlytRNA-upregulating plasmid produced an additional ~2-fold increase relative to the AKTK construct alone, yielding a cumulative 17.0-fold improvement (124.9 ± 20.2 mg L^{-1}) compared to the baseline plasmid (Fig. S9b and S11). Additionally, RT-qPCR results provided strong evidence that translation was the primary bottleneck in S8E58-K expression. In fact, the fold of induction of the S8E58-K transcript was higher for the baseline construct, indicating that transcription was not the limiting step (Fig. S12). Thus, our results suggest that the N-terminal tag alone alleviated a translation barrier, creating conditions for additional strategies (*e.g.*, GlytRNA upregulation) to become effective too. This showed how optimising S8E58-K production required targeting the most limiting step first (*i.e.*, translation) before other modifications could provide additional benefits. Collectively, these findings identify N-terminal engineering as a powerful entry point for improving SELP yields. Consequently, subsequent protein variants in this study incorporated the AKTK N-terminal tag.

- *Silk-like block redistribution:* previous studies showed that variations in the number of silk-like blocks in fusion proteins

containing also thermoresponsive blocks (elastin-like or resilin-like) influenced their productivity, albeit with contradictory results. While Machado *et al.* reported increased yields (from 151 to 198 mg L^{-1}) by reducing the silk-to-elastin ratio,[30] Huang *et al.* reported a reduction in yields for resilin–silk-like polypeptides (from 85 to 63 mg L^{-1}) by increasing the number of consecutive silk-like blocks from 2 to 8.[72] We hypothesised that silk-like blocks could promote premature intracellular SELP aggregation *via* the formation of interprotein β-sheets, and that reducing the number of consecutive silk-like blocks could limit this effect, thereby alleviating the metabolic burden on the host cell, reducing stress and irreversible aggregation, and overall enhancing soluble SELP expression.[13,73,74] To test this, we designed a S8E58-K variant, termed S4E58-K (also incorporating an N-terminal AKTK tag). Unlike previous studies that changed the overall silk-to-elastin ratio by varying the total number of silk-like blocks, our strategy focused on varying block positioning – we kept the same total number of silk-like blocks in S4E58-K and S8E58-K but varied their distribution along the sequence (4 consecutive silk-like blocks in S4E58-K *vs.* 8 in S8E58-K).

Contrary to our hypothesis, expression levels of S4E58-K and S8E58-K produced comparable yields (Fig. S9c and S13), with no statistically significant difference between the two constructs (62.3 ± 9.9 and 62.06 ± 10.5, respectively). These results indicated that, under the tested conditions, premature β-sheet aggregation due to silk-like block clustering was not a major cause of reduced yield. In fact, the lack of a measurable yield benefit suggests that, under the tested conditions, both S8E58-K and S4E58-K remained below the aggregation threshold during protein expression. It is therefore possible that the hypothesised benefits of reduced consecutive silk-like blocks may only become apparent under conditions that impose greater host stress, such as higher consecutive blocks, higher expression levels, extended induction times or altered temperature regimes.[75]

Overall, these findings point out that the combination of T7-driven expression, AKTK tagging, and GlytRNA supplementation likely established a ceiling for translation initiation and elongation, limiting the effect of subsequent sequence-level changes. The 17.0-fold increase achieved in this study from the baseline construct represents a substantial improvement within these constraints.

- *Reduced molecular weight plus silk-like block redistribution:* a lower MW SELP variant with a maximum of two consecutive silk-like blocks (S2E39-K) was engineered. This was motivated by the known negative correlation between protein MW and soluble expression in *E. coli*.[60,76–78] Additionally, the number of clustered silk-like blocks was reduced, as it has been reported that increasing genetic repeat number in silk-like proteins can compromise plasmid stability, reducing maintenance by up to 75% in high-density cultures and thereby lowering protein yields.[58] However, no positive effects were observed from the reduction in MW or the reduced number of consecutive silk-like blocks. Compared to the baseline construct, the yields for S2E39-K increased by 9.2-fold (67.9 ± 8.9 mg L^{-1}), attaining similar levels than S8E58-K or S4E58-K after inserting the AKTK (Fig. 4 and S14). Therefore, these results reinforced the positive impact of the N-terminal AKTK tag. Importantly, the reduced MW might negatively impact the material properties of S2E39-K-derived materials, as shorter protein chains lead to reduced intermolecular entanglements and weaker mechanical properties.[14,79] Therefore, while MW reduction might be a valid yield optimisation strategy, it must be balanced against potential losses in material performance, particularly when downstream applications require high mechanical strength and durability.

Discussion

This study systematically analysed the effect of various bioprocessing parameters, plasmid backbone modifications and protein engineering strategies on the recombinant yields of three SELPs. Initial tests focused on optimisation of bioprocessing conditions (temperature, *E. coli* strain and IPTG concentration) for S8E58-K did not result in statistically significant differences in protein yield. Therefore, subsequent experiments focused on plasmid backbone modifications and protein engineering strategies.

Statistical comparison across the different constructs tested, including means, 95% confidence intervals, Welch's *t*-tests and effect sizes can be found in Table S6. Plasmid backbone modifications alone (constructs S8E58-K_T7_Amp, S8E58-K_T7_Kan, S8E58-K_pBAD_Kan and pACYC184_glyVXY) led to consistently low yields, accompanied by wide 95% confidence intervals and no statistically significant differences with respect to the baseline construct. This reflected substantial uncertainty due to the limited sample size ($n = 3$) and suggested that plasmid backbone changes were insufficient to overcome the expression bottlenecks for S8E58-K. In contrast, incorporating a N-terminal AKTK tag (construct AKTK_S8E58-K_ T7_Kan) led to a marked and statistically significant increase in SELP yields ($p < 0.01$) relative to the baseline construct. Incorporating an N-terminal AKTK tag increased S8E58-K expression roughly 8.5-fold, while RT-qPCR data suggested that this tag was alleviating a translational rather than transcriptional limitation. Importantly, this effect was largely independent of protein MW and silk-like block architecture (constructs AKTK_S4E58-K_T7_Amp and AKTK_S2E39-K_ T7_Amp), underscoring the dominant role of N-terminal sequence features in controlling translational throughput for repetitive, aggregation-prone polypeptides.

The higher ribosome throughput caused by the AKTK tag exposed a second bottleneck: the unusually high demand for glycine incorporation required for a protein composed of *ca.* 40% glycine. Under the higher translational efficiency provided by the AKTK tag, GlytRNA upregulation led to an additional ~2-fold yield increase. These results highlighted the convoluted nature of translational limitations in SELP

expression, underscoring how protein-level engineering can simultaneously enable more effective plasmid backbone interventions.

Our optimal conditions (combining N-terminal AKTK tag with GlytRNA upregulation) achieved a yield of 124.9 ± 20.2 mg L^{-1}, which is among the highest reported so far for SELPs produced in shake flasks (Table S1). Our yields, however, are lower than those reported in bioreactors, which are not directly comparable to shake-flask experiments due to the enhanced control over oxygen transfer, pH, and feeding strategies in bioreactors. Bioreactors generally lead to higher cell densities and productivities, and hence we would anticipate that further optimisation in bioreactors could lead to even higher yields for the SELPs reported in this study.

Incorporating an N-terminal AKTK tag has since improved the yields of several other SELPs in our lab by up to 2 orders of magnitude, demonstrating the generalisability of the approach reported in this work. Thus, we expect that N-terminal sequence design could alleviate expression bottlenecks in SELPs and other protein-based biomaterials, a key step towards developing commercially viable protein-based materials. Furthermore, higher SELP yields may also facilitate the development of new downstream chemical or enzymatic modification strategies that expand the functionality and design space of SELP-based materials, such as lipidated or other post-translationally modified derivatives.

Conclusion

SELPs are recombinant structural protein biopolymers that have attracted significant interest due to their inherently sustainable nature, tuneable properties, and ability to self-assemble into robust materials in response to stimuli such as temperature or pH, making them promising substitutes for fossil-based polymers across diverse fields.[19,20,80] Unfortunately, yields for recombinant structural proteins remain relatively low, representing a major hurdle for the commercial viability of these biopolymers. To that end, this study systematically evaluated bioprocess engineering, plasmid backbone and protein engineering strategies to enhance SELP expression in *E. coli*, identifying both opportunities and constraints for optimising their yields. Across successive rounds of engineering, the yields of SELPs were pushed toward higher values. Among the different modifications tested, the incorporation of a translation-enhancing AKTK tag after the start codon at the N-terminus proved the most successful: the yield of S8E58-K was enhanced by 8.5-fold with respect to the baseline construct (from 7.3 ± 3.1 to 62.3 ± 9.9 mg L^{-1}). This and RT qPCR results indicated that the bottleneck for SELP expression was protein translation in this case. Subsequently, other approaches (*i.e.*, upregulation of GlytRNA) increased the yields further, leading to a cumulative 17.0-fold increase in S8E58-K productivity relative to the baseline construct, up to 124.9 ± 20.2 mg L^{-1}. Other protein engineering modifications that also incorporated the AKTK tag, namely a reduction in MW and a redistribution of silk-like blocks, did not lead to further increases, underscoring the critical role of translation initiation in the production of recombinant SELPs.

Conflicts of interest

There are no conflicts to declare.

Data availability

The data supporting this article have been included as part of the supplementary information (SI): literature review, full list of SELP sequences, primers and plasmid constructs used in this study, as well as productivity data for individual protein production runs. Figures include plasmid maps, MALDI-TOF MS results, RT-qPCR data, glycine codon usage profiles, additional SDS PAGE gels and dry weight yields. See DOI: https://doi.org/10.1039/d6me00011h.

Acknowledgements

DLB acknowledges financial support from UK Research and Innovation (UKRI) *via* the Engineering and Physical Sciences Research Council (EPSRC) New Investigator Award (UKRI128). The Jack Jeffries lab at UCL is acknowledge for providing the *E. coli* BW25113 strain. Dr Kersti Keru (UCL Chemistry Mass Spectrometry Facility) is acknowledged for the assistance with MALDI-TOF MS experiments.

References

1 *Marine Anthropogenic Litter*, ed. M. Bergmann, L. Gutow and M. Klages, Springer International Publishing, Cham, 2015, DOI: 10.1007/978-3-319-16510-3.
2 The Business Research Company, How will the synthetic polymers market grow? key trends and opportunities for 2025 and beyond, Latest Global Market Insights, https://blog.tbrc.info/2025/02/synthetic-polymers-market-demand/, (accessed 2025-07-04).
3 H. Agnieray, J. L. Glasson, Q. Chen, M. Kaur and L. J. Domigan, Recent Developments in Sustainably Sourced Protein-Based Biomaterials, *Biochem. Soc. Trans.*, 2021, **49**(2), 953–964, DOI: 10.1042/BST20200896.
4 S. Ling, D. L. Kaplan and M. J. Buehler, Nanofibrils in Nature and Materials Engineering, *Nat. Rev. Mater.*, 2018, **3**(4), 18016, DOI: 10.1038/natrevmats.2018.16.
5 A. Agarwal, B. Shaida, M. Rastogi and N. B. Singh, Food Packaging Materials with Special Reference to Biopolymers-Properties and Applications, *Chem. Afr.*, 2023, **6**(1), 117–144, DOI: 10.1007/s42250-022-00446-w.
6 H. Iyer, P. Grandgeorge, A. M. Jimenez, I. R. Campbell, M. Parker, M. Holden, M. Venkatesh, M. Nelsen, B. Nguyen and E. Roumeli, Fabricating Strong and Stiff Bioplastics from Whole Spirulina Cells, *Adv. Funct. Mater.*, 2023, **33**(40), 2302067, DOI: 10.1002/adfm.202302067.

7 Z. Wang, H. Wei, Y. Huang, Y. Wei and J. Chen, Naturally Sourced Hydrogels: Emerging Fundamental Materials for next-Generation Healthcare Sensing, *Chem. Soc. Rev.*, 2023, **52**(9), 2992–3034, DOI: 10.1039/D2CS00813K.

8 C. Yang, H. Wang, K. Wang, Z. Cao, F. Ren, G. Zhou, Y. Chen and B. Sun, Silk Fibroin-Based Biomemristors for Bionic Artificial Intelligence Robot Applications, *ACS Nano*, 2025, **19**(18), 17173–17198, DOI: 10.1021/acsnano.5c02480.

9 H. Zhao, B. Yu, D. Yu, T. Ji, K. Nie, J. Tian, X. Shen, K. Zhang, J. Ou, X. Yang, D. Xiao, Q. Zhou and W. Huang, Electrochemical-genetic Programming of Protein-based Magnetic Soft Robots for Active Drug Delivery, *Adv. Sci.*, 2025, 2503404, DOI: 10.1002/advs.202503404.

10 D. López Barreiro, I. J. Minten, J. C. Thies and C. M. J. Sagt, Structure–Property Relationships of Elastin-like Polypeptides: A Review of Experimental and Computational Studies, *ACS Biomater. Sci. Eng.*, 2023, **9**(7), 3796–3809, DOI: 10.1021/acsbiomaterials.1c00145.

11 S. Roberts, M. Dzuricky and A. Chilkoti, Elastin-like Polypeptides as Models of Intrinsically Disordered Proteins, *FEBS Lett.*, 2015, **589**(19 Part A), 2477–2486, DOI: 10.1016/j.febslet.2015.08.029.

12 W. Qiu, Y. Huang, W. Teng, C. M. Cohn, J. Cappello and X. Wu, Complete Recombinant Silk-Elastinlike Protein-Based Tissue Scaffold, *Biomacromolecules*, 2010, **11**(12), 3219–3227, DOI: 10.1021/bm100469w.

13 J. A. Gustafson and H. Ghandehari, Silk-Elastinlike Protein Polymers for Matrix-Mediated Cancer Gene Therapy, *Adv. Drug Delivery Rev.*, 2010, **62**(15), 1509–1523, DOI: 10.1016/j.addr.2010.04.006.

14 K. J. Isaacson, M. M. Jensen, A. H. Watanabe, B. E. Green, M. A. Correa, J. Cappello and H. Ghandehari, Self-assembly of Thermoresponsive Recombinant Silk-elastinlike Nanogels, *Macromol. Biosci.*, 2018, **18**(1), 1700192, DOI: 10.1002/mabi.201700192.

15 L. Chambre, Z. Martín-Moldes, R. N. Parker and D. L. Kaplan, Bioengineered Elastin- and Silk-Biomaterials for Drug and Gene Delivery, *Adv. Drug Delivery Rev.*, 2020, **160**, 186–198, DOI: 10.1016/j.addr.2020.10.008.

16 W. Huang, A. Rollett and D. L. Kaplan, Silk-Elastin-like Protein Biomaterials for the Controlled Delivery of Therapeutics, *Expert Opin. Drug Delivery*, 2015, **12**(5), 779–791, DOI: 10.1517/17425247.2015.989830.

17 F. Cipriani, M. Krüger, I. G. de Torre, L. Q. Sierra, M. A. Rodrigo, L. Kock and J. C. Rodriguez-Cabello, Cartilage Regeneration in Preannealed Silk Elastin-Like Co-Recombinamers Injectable Hydrogel Embedded with Mature Chondrocytes in an Ex Vivo Culture Platform, *Biomacromolecules*, 2018, **19**(11), 4333–4347, DOI: 10.1021/acs.biomac.8b01211.

18 Z. Martín-Moldes, Q. Spey, T. Bhatacharya and D. L. Kaplan, Silk-elastin-like-protein/Graphene-oxide Composites for Dynamic Electronic Biomaterials, *Macromol. Biosci.*, 2022, **22**(8), 2200122, DOI: 10.1002/mabi.202200122.

19 H. Shi, T. Ji, C. Zhai, J. Lu, W. Huang and J. Yeo, Thermo- and Ion-Responsive Silk-Elastin-like Proteins and Their Multiscale Mechanisms, *J. Mater. Chem. B*, 2022, **10**(32), 6133–6142, DOI: 10.1039/D2TB01002J.

20 O. P. Narayan, X. Mu, O. Hasturk and D. L. Kaplan, Dynamically Tunable Light Responsive Silk-Elastin-like Proteins, *Acta Biomater.*, 2021, **121**, 214–223, DOI: 10.1016/j.actbio.2020.12.018.

21 D. E. Meyer and A. Chilkoti, Purification of Recombinant Proteins by Fusion with Thermally-Responsive Polypeptides, *Nat. Biotechnol.*, 1999, **17**(11), 1112–1115, DOI: 10.1038/15100.

22 K. Schacht and T. Scheibel, Processing of Recombinant Spider Silk Proteins into Tailor-Made Materials for Biomaterials Applications, *Curr. Opin. Biotechnol.*, 2014, **29**, 62–69, DOI: 10.1016/j.copbio.2014.02.015.

23 M. Humenik, K. Pawar and T. Scheibel, Nanostructured, Self-Assembled Spider Silk Materials for Biomedical Applications, in *Biological and Bio-inspired Nanomaterials*, ed. S. Perrett, A. K. Buell and T. P. J. Knowles, Advances in Experimental Medicine and Biology, Springer Singapore, Singapore, 2019, vol. 1174, pp. 187–221, DOI: 10.1007/978-981-13-9791-2_6.

24 M. Bzymek and S. T. Lovett, Instability of Repetitive DNA Sequences: The Role of Replication in Multiple Mechanisms, *Proc. Natl. Acad. Sci. U. S. A.*, 2001, **98**(15), 8319–8325, DOI: 10.1073/pnas.111008398.

25 K. Kim, D. Choe, D.-H. Lee and B.-K. Cho, Engineering Biology to Construct Microbial Chassis for the Production of Difficult-to-Express Proteins, *Int. J. Mol. Sci.*, 2020, **21**(3), 990, DOI: 10.3390/ijms21030990.

26 C. H. Bowen, B. Dai, C. J. Sargent, W. Bai, P. Ladiwala, H. Feng, W. Huang, D. L. Kaplan, J. M. Galazka and F. Zhang, Recombinant Spidroins Fully Replicate Primary Mechanical Properties of Natural Spider Silk, *Biomacromolecules*, 2018, **19**(9), 3853–3860, DOI: 10.1021/acs.biomac.8b00980.

27 G. Bhattacharyya, P. Oliveira, S. T. Krishnaji, D. Chen, M. Hinman, B. Bell, T. I. Harris, A. Ghazitabatabaei, R. V. Lewis and J. A. Jones, Large Scale Production of Synthetic Spider Silk Proteins in Escherichia Coli, *Protein Expression Purif.*, 2021, **183**, 105839, DOI: 10.1016/j.pep.2021.105839.

28 T. Collins, M. Barroca, F. Branca, J. Padrão, R. Machado and M. Casal, High Level Biosynthesis of a Silk-Elastin-like Protein in E. Coli, *Biomacromolecules*, 2014, **15**(7), 2701–2708, DOI: 10.1021/bm5005564.

29 M. Barroca, P. Rodrigues, R. Sobral, M. M. R. Costa, S. R. Chaves, R. Machado, M. Casal and T. Collins, Antibiotic Free Selection for the High Level Biosynthesis of a Silk-Elastin-like Protein, *Sci. Rep.*, 2016, **6**(1), 39329, DOI: 10.1038/srep39329.

30 R. Machado, J. Azevedo-Silva, C. Correia, T. Collins, F. J. Arias, J. C. Rodríguez-Cabello and M. Casal, High Level Expression and Facile Purification of Recombinant Silk-Elastin-like Polymers in Auto Induction Shake Flask Cultures, *AMB Express*, 2013, **3**(1), 11, DOI: 10.1186/2191-0855-3-11.

31 Q. Wang, X. Xia, W. Huang, Y. Lin, Q. Xu and D. L. Kaplan, High Throughput Screening of Dynamic Silk-elastin-like Protein Biomaterials, *Adv. Funct. Mater.*, 2014, **24**(27), 4303–4310, DOI: 10.1002/adfm.201304106.

32 C. Gonzalez-Obeso, J. C. Rodriguez-Cabello and D. L. Kaplan, Fast and Reversible Crosslinking of a Silk Elastin-like Polymer, *Acta Biomater.*, 2022, **141**, 14–23, DOI: 10.1016/j.actbio.2021.12.031.

33 A. Ibáñez-Fonseca, D. Orbanic, F. J. Arias, M. Alonso, D. I. Zeugolis and J. C. Rodríguez-Cabello, Influence of the Thermodynamic and Kinetic Control of Self-assembly on the Microstructure Evolution of Silk-elastin-like Recombinamer Hydrogels, *Small*, 2020, **16**(28), 2001244, DOI: 10.1002/smll.202001244.

34 D. López Barreiro, A. Folch-Fortuny, I. Muntz, J. C. Thies, C. M. J. Sagt and G. H. Koenderink, Sequence Control of the Self-Assembly of Elastin-Like Polypeptides into Hydrogels with Bespoke Viscoelastic and Structural Properties, *Biomacromolecules*, 2023, **24**(1), 489–501, DOI: 10.1021/acs.biomac.2c01405.

35 D. López Barreiro, K. Houben, O. Schouten, G. H. Koenderink, J. C. Thies and C. M. J. Sagt, Order–Disorder Balance in Silk-Elastin-like Polypeptides Determines Their Self-Assembly into Hydrogel Networks, *ACS Appl. Mater. Interfaces*, 2025, **17**(1), 650–662, DOI: 10.1021/acsami.4c17903.

36 T. Collins, J. Azevedo-Silva, A. Da Costa, F. Branca, R. Machado and M. Casal, Batch Production of a Silk-Elastin-like Protein in E. Coli BL21(DE3): Key Parameters for Optimisation, *Microb. Cell Fact.*, 2013, **12**(1), 21, DOI: 10.1186/1475-2859-12-21.

37 A. Miserez, J. Yu and P. Mohammadi, Protein-Based Biological Materials: Molecular Design and Artificial Production, *Chem. Rev.*, 2023, **123**(5), 2049–2111, DOI: 10.1021/acs.chemrev.2c00621.

38 O. Tokareva, V. A. Michalczechen-Lacerda, E. L. Rech and D. L. Kaplan, Recombinant DNA Production of Spider Silk Proteins, *Microb. Biotechnol.*, 2013, **6**(6), 651–663, DOI: 10.1111/1751-7915.12081.

39 T. Scheibel, Spider Silks: Recombinant Synthesis, Assembly, Spinning, and Engineering of Synthetic Proteins, *Microb. Cell Fact.*, 2004, **3**(1), 14, DOI: 10.1186/1475-2859-3-14.

40 M. A. Morris, R. A. Bataglioli, D. J. Mai, Y. J. Yang, J. M. Paloni, C. E. Mills, Z. D. Schmitz, E. A. Ding, A. C. Huske and B. D. Olsen, Democratizing the Rapid Screening of Protein Expression for Materials Development, *Mol. Syst. Des. Eng.*, 2023, **8**(2), 227–239, DOI: 10.1039/D2ME00150K.

41 L. Bivona, Z. Zou, N. Stutzman and P. D. Sun, Influence of the Second Amino Acid on Recombinant Protein Expression, *Protein Expression Purif.*, 2010, **74**(2), 248–256, DOI: 10.1016/j.pep.2010.06.005.

42 A. Connor, C. Wigham, Y. Bai, M. Rai, S. Nassif, M. Koffas and R. H. Zha, Novel Insights into Construct Toxicity, Strain Optimization, and Primary Sequence Design for Producing Recombinant Silk Fibroin and Elastin-like Peptide in E. Coli, *Metab. Eng. Commun.*, 2023, **16**, e00219, DOI: 10.1016/j.mec.2023.e00219.

43 J. Kyte and R. F. Doolittle, A Simple Method for Displaying the Hydropathic Character of a Protein, *J. Mol. Biol.*, 1982, **157**(1), 105–132, DOI: 10.1016/0022-2836(82)90515-0.

44 E. Gasteiger, A. Gattiker, C. Hoogland, I. Ivanyi, R. D. Appel and A. Bairoch, ExPASy: The Proteomics Server for in-Depth Protein Knowledge and Analysis, *Nucleic Acids Res.*, 2003, **31**(13), 3784–3788, DOI: 10.1093/nar/gkg563.

45 W. P. Tate, Termination of Polypeptide Synthesis, in *Peptide and Protein Reviews*, Plenum Press, New York, 1984, vol. 2, pp. 173–208.

46 X.-X. Xia, Z.-G. Qian, C. S. Ki, Y. H. Park, D. L. Kaplan and S. Y. Lee, Native-Sized Recombinant Spider Silk Protein Produced in Metabolically Engineered Escherichia Coli Results in a Strong Fiber, *Proc. Natl. Acad. Sci. U. S. A.*, 2010, **107**(32), 14059–14063, DOI: 10.1073/pnas.1003366107.

47 D. T. McPherson, J. Xu and D. W. Urry, Product Purification by Reversible Phase Transition Following Escherichia Coli Expression of Genes Encoding up to 251 Repeats of the Elastomeric pentapeptide GVGVP, *Protein Expression Purif.*, 1996, **7**(1), 51–57, DOI: 10.1006/prep.1996.0008.

48 M. Navarro and J. A. Planell, Nanotechnology in Regenerative Medicine: Methods and Protocols, *Methods in Molecular Biology, Methods and Protocols*, Humana Press, Totowa, NJ, 2012, DOI: 10.1007/978-1-61779-388-2.

49 J. C. Rodríguez-Cabello, A. Girotti, A. Ribeiro and F. J. Arias, Synthesis of Genetically Engineered Protein Polymers (Recombinamers) as an Example of Advanced Self-Assembled Smart Materials, in *Nanotechnology in Regenerative Medicine*, Methods in Molecular Biology, ed. M. Navarro and J. A. Planell, Humana Press, 2012, vol. 811(2), pp. 17–38, DOI: 10.1007/978-1-61779-388-2_2.

50 E. J. Hartzell, C. Gonzalez Obeso, O. Hasturk, R. A. Scheel, L. Wan, F. Moser, T. Smith and D. Kaplan, Exploration of Stimuli-responsive, Elastin-based Coatings for Textiles, *Adv. Funct. Mater.*, 2025, **35**(15), 2407882, DOI: 10.1002/adfm.202407882.

51 J. Schindelin, I. Arganda-Carreras, E. Frise, V. Kaynig, M. Longair, T. Pietzsch, S. Preibisch, C. Rueden, S. Saalfeld, B. Schmid, J.-Y. Tinevez, D. J. White, V. Hartenstein, K. Eliceiri, P. Tomancak and A. Cardona, Fiji: An Open-Source Platform for Biological-Image Analysis, *Nat. Methods*, 2012, **9**(7), 676–682, DOI: 10.1038/nmeth.2019.

52 R. Rudolph and H. Lilie, In Vitro Folding of Inclusion Body Proteins, *FASEB J.*, 1996, **10**(1), 49–56, DOI: 10.1096/fasebj.10.1.8566547.

53 L. F. Vallejo and U. Rinas, Strategies for the Recovery of Active Proteins through Refolding of Bacterial Inclusion Body Proteins, *Microb. Cell Fact.*, 2004, **3**(1), 11, DOI: 10.1186/1475-2859-3-11.

54 B. Fischer, B. Perry, I. Sumner and P. Goodenough, A Novel Sequential Procedure to Enhance the Renaturation of Recombinant Protein from Escherichia Coli Inclusion Bodies, *Protein Eng., Des. Sel.*, 1992, **5**(6), 593–596, DOI: 10.1093/protein/5.6.593.

55 Escherichia Coli 16S rRNA Gene, Strain BL21, 2004, http://www.ncbi.nlm.nih.gov/nuccore/AJ605115.1, (accessed 2026-05-08).

56 K. J. Livak and T. D. Schmittgen, Analysis of Relative Gene Expression Data Using Real-Time Quantitative PCR and the

2−ΔΔCT Method, *Methods*, 2001, **25**(4), 402–408, DOI: 10.1006/meth.2001.1262.

57 B. L. Welch, The Generalization of `student's' Problem When Several Different Population Variances Are Involved, *Biometrika*, 1947, **34**(1/2), 28, DOI: 10.2307/2332510.

58 Y.-X. Yang, Z.-G. Qian, J.-J. Zhong and X.-X. Xia, Hyper-Production of Large Proteins of Spider Dragline Silk MaSp2 by Escherichia Coli via Synthetic Biology Approach, *Process Biochem.*, 2016, **51**(4), 484–490, DOI: 10.1016/j.procbio.2016.01.006.

59 V. Gupta and J. E. Dick, Real-Time Intracellular Analysis of Kanamycin Using Microaptasensors, *ACS Sens.*, 2023, **8**(3), 1143–1150, DOI: 10.1021/acssensors.2c02427.

60 R. V. Lewis, M. Hinman, S. Kothakota and M. J. Fournier, Expression and Purification of a Spider Silk Protein: A New Strategy for Producing Repetitive Proteins, *Protein Expression Purif.*, 1996, **7**(4), 400–406, DOI: 10.1006/prep.1996.0060.

61 N. Lee, C. Francklyn and E. P. Hamilton, Arabinose-Induced Binding of AraC Protein to araI2 Activates the araBAD Operon Promoter, *Proc. Natl. Acad. Sci. U. S. A.*, 1987, **84**(24), 8814–8818, DOI: 10.1073/pnas.84.24.8814.

62 S. Balzer, V. Kucharova, J. Megerle, R. Lale, T. Brautaset and S. Valla, A Comparative Analysis of the Properties of Regulated Promoter Systems Commonly Used for Recombinant Gene Expression in Escherichia Coli, *Microb. Cell Fact.*, 2013, **12**, 26, DOI: 10.1186/1475-2859-12-26.

63 G. C. Candelas, G. Arroyo, C. Carrasco and R. Dompenciel, Spider Silkglands Contain a Tissue-Specific Alanine tRNA That Accumulates in Vitro in Response to the Stimulus for Silk Protein Synthesis, *Dev. Biol.*, 1990, **140**(1), 215–220, DOI: 10.1016/0012-1606(90)90069-U.

64 A. Heidebrecht and T. Scheibel, Recombinant Production of Spider Silk Proteins, in *Advances in Applied Microbiology*, Elsevier, 2013, vol. 82, pp. 115–153, DOI: 10.1016/B978-0-12-407679-2.00004-1.

65 H. Gingold and Y. Pilpel, Determinants of Translation Efficiency and Accuracy, *Mol. Syst. Biol.*, 2011, **7**(1), 481, DOI: 10.1038/msb.2011.14.

66 K. C. Stein and J. Frydman, The Stop-and-Go Traffic Regulating Protein Biogenesis: How Translation Kinetics Controls Proteostasis, *J. Biol. Chem.*, 2019, **294**(6), 2076–2084, DOI: 10.1074/jbc.REV118.002814.

67 X. Jia, X. He, C. Huang, J. Li, Z. Dong and K. Liu, Protein Translation: Biological Processes and Therapeutic Strategies for Human Diseases, *Signal Transduction Targeted Ther.*, 2024, **9**(1), 44, DOI: 10.1038/s41392-024-01749-9.

68 C. Gonzalez-Obeso, F. G. Backlund and D. L. Kaplan, Charge-Modulated Accessibility of Tyrosine Residues for Silk-Elastin Copolymer Cross-Linking, *Biomacromolecules*, 2022, **23**(3), 760–765, DOI: 10.1021/acs.biomac.1c01192.

69 E. Kim, B. Dai, J. B. Qiao, W. Li, J. D. Fortner and F. Zhang, Microbially Synthesized Repeats of Mussel Foot Protein Display Enhanced Underwater Adhesion, *ACS Appl. Mater. Interfaces*, 2018, **10**(49), 43003–43012, DOI: 10.1021/acsami.8b14890.

70 E. Kim, J. Jeon, Y. Zhu, E. D. Hoppe, Y.-S. Jun, G. M. Genin and F. Zhang, A Biosynthetic Hybrid Spidroin-Amyloid-Mussel Foot Protein for Underwater Adhesion on Diverse Surfaces, *ACS Appl. Mater. Interfaces*, 2021, **13**(41), 48457–48468, DOI: 10.1021/acsami.1c14182.

71 A. Tats, M. Remm and T. Tenson, Highly Expressed Proteins Have an Increased Frequency of Alanine in the Second Amino Acid Position, *BMC Genomics*, 2006, **7**(1), 28, DOI: 10.1186/1471-2164-7-28.

72 S.-C. Huang, R.-X. Fan, K.-K. Tian, X.-X. Xia and Z.-G. Qian, Controllable Fibrillization Reinforces Genetically Engineered Rubberlike Protein Hydrogels, *Biomacromolecules*, 2021, **22**(2), 961–970, DOI: 10.1021/acs.biomac.0c01653.

73 O. S. Tokareva, S. Lin, M. M. Jacobsen, W. Huang, D. Rizzo, D. Li, M. Simon, C. Staii, P. Cebe, J. Y. Wong, M. J. Buehler and D. L. Kaplan, Effect of Sequence Features on Assembly of Spider Silk Block Copolymers, *J. Struct. Biol.*, 2014, **186**(3), 412–419, DOI: 10.1016/j.jsb.2014.03.004.

74 R. Dandu, A. V. Cresce, R. Briber, P. Dowell, J. Cappello and H. Ghandehari, Silk–Elastinlike Protein Polymer Hydrogels: Influence of Monomer Sequence on Physicochemical Properties, *Polymer*, 2009, **50**(2), 366–374, DOI: 10.1016/j.polymer.2008.11.047.

75 S. Sosa-Carrillo, H. Galez, S. Napolitano, F. Bertaux and G. Batt, Maximizing Protein Production by Keeping Cells at Optimal Secretory Stress Levels Using Real-Time Control Approaches, *Nat. Commun.*, 2023, **14**(1), 3028, DOI: 10.1038/s41467-023-38807-9.

76 J. T. Prince, K. P. McGrath, C. M. DiGirolamo and D. L. Kaplan, Construction, Cloning, and Expression of Synthetic Genes Encoding Spider Dragline Silk, *Biochemistry*, 1995, **34**(34), 10879–10885, DOI: 10.1021/bi00034a022.

77 H. Chung, T. Y. Kim and S. Y. Lee, Recent Advances in Production of Recombinant Spider Silk Proteins, *Curr. Opin. Biotechnol.*, 2012, **23**(6), 957–964, DOI: 10.1016/j.copbio.2012.03.013.

78 A. M. Edlund, J. Jones, R. Lewis and J. C. Quinn, Economic Feasibility and Environmental Impact of Synthetic Spider Silk Production from Escherichia Coli, *New Biotechnol.*, 2018, **42**, 12–18, DOI: 10.1016/j.nbt.2017.12.006.

79 X.-X. Xia, Q. Xu, X. Hu, G. Qin and D. L. Kaplan, Tunable Self-Assembly of Genetically Engineered Silk–Elastin-like Protein Polymers, *Biomacromolecules*, 2011, **12**(11), 3844–3850, DOI: 10.1021/bm201165h.

80 Y. Noh, E. Son and C. Cha, Exploring Stimuli-Responsive Elastin-like Polypeptide for Biomedicine and beyond: Potential Application as Programmable Soft Actuators, *Front. Bioeng. Biotechnol.*, 2023, **11**, 1284226, DOI: 10.3389/fbioe.2023.1284226.